

1 **Reconstructing the annual mass balance of glacier Echaurren Norte (Central Andes,**
2 **33.5°S) using local and regional hydro-climatic data**

3

4 **M.H. Masiokas^{1*}, D.A. Christie^{2,3}, C. Le Quesne², P. Pitte¹, L. Ruiz¹, R. Villalba¹, B.H.**
5 **Luckman⁴, E. Berthier⁵, S.U. Nussbaumer⁶, A. González-Reyes⁷, J. McPhee⁸, G. Barcaza⁹**

6

7 ¹ Instituto Argentino de Nivología, Glaciología y Ciencias Ambientales (IANIGLA),

8 CCT- CONICET Mendoza, C.C. 330, (5500) Mendoza, Argentina

9 ² Laboratorio de Dendrocronología y Cambio Global, Instituto de Conservación Biodiversidad y

10 Territorio, Facultad de Ciencias Forestales y Recursos Naturales, Universidad Austral de Chile,

11 Valdivia, Chile.

12 ³ Center for Climate and Resilience Research (CR)², Chile.

13 ⁴ Department of Geography, University of Western Ontario, Canada.

14 ⁵ LEGOS, CNRS, Université de Toulouse, France

15 ⁶ Department of Geography, University of Zurich, and Department of Geosciences, University of

16 Fribourg, Switzerland.

17 ⁷ Departamento de Geología, Facultad de Ciencias Físicas y Matemáticas, Universidad de Chile.

18 ⁸ Departamento de Ingeniería Civil, Facultad de Ciencias Físicas y Matemáticas, Universidad de

19 Chile.

20 ⁹ Dirección General de Aguas (DGA), Santiago, Chile.

21

22 * Correspondence to: mmasiokas@mendoza-conicet.gob.ar

23 Tel.: +54-261-5244264

24 Fax: +54-261-5244201

25

26 **Abstract**

27 Despite the great number and variety of glaciers in southern South America, *in situ* glacier mass
28 balance records are extremely scarce and glacier-climate relationships are still poorly understood
29 in this region. Here we use the longest (>35 yrs) and most complete *in situ* mass balance record,
30 available for glacier Echaurren Norte in the Andes at ~33.5°S, to develop a minimal glacier
31 surface mass balance model that relies on nearby monthly precipitation and air temperature data
32 as forcing. This basic model is able to explain 78% of the variance in the annual glacier mass
33 balance record over the 1978-2013 calibration period. An attribution assessment identified
34 precipitation variability as the dominant forcing modulating annual mass balances at ECH, with
35 temperature variations likely playing a secondary role. A regionally-averaged series of mean
36 annual streamflow records from both sides of the Andes is then used to estimate, through simple
37 linear regression, this glacier's annual mass balance variations since 1909. The reconstruction
38 model captures 68% of the observed glacier mass balance variability and shows three periods of
39 sustained positive mass balances embedded in an overall negative trend over the past 105 years.
40 The three periods of sustained positive mass balances (centered in the 1920s-30s, in the 1980s
41 and in the first decade of the 21st century) coincide with several documented glacier advances in
42 this region. Similar trends observed in other shorter glacier mass balance series suggest that the
43 glacier Echaurren Norte reconstruction is representative of larger-scale conditions and could be
44 useful for more detailed glaciological, hydrological and climatological assessments in this portion
45 of the Andes.

46

47 **1. Introduction**

48 The extra-tropical Andes between $\sim 23^\circ$ and 55°S contain a large number and variety of glaciers
49 ranging from small glacierets at elevations of over 6000 m in the high, arid Andes of northern
50 Chile and Argentina, to large outlet glaciers that reach the sea in the humid southwestern portion
51 of Patagonia and Tierra del Fuego. Altogether, these ice masses concentrate the largest
52 glacierized area in the Southern Hemisphere outside Antarctica and are highly valued as sources
53 of freshwater, as indicators of climatic change, as tourist attractions, and as environmental and
54 cultural icons in different sectors of the Andes. As reported for other mountainous areas of the
55 globe, glaciers in southern South America display a widespread retreating pattern that has been
56 usually attributed to warmer, and sometimes drier, climatic conditions in this region (Villalba et
57 al. 2003; Rignot et al. 2003; Rivera et al. 2000, 2005; Masiokas et al. 2008, 2009; Le Quesne et
58 al. 2009; Pellicciotti et al. 2014). Quantitative assessments of regional glacier mass balance
59 changes and glacier-climate relationships are, however, seriously hampered by the scarcity and
60 short length of *in situ* glacier mass balance data and proximal climate records within the Andes.
61 The latest publication of the World Glacier Monitoring Service (WGMS 2013) reports annual
62 mass balance measurements for seven extratropical Andean glaciers (five in Argentina, two in
63 Chile). Four of these records start in 2010 and are for small glaciers and glacierets located ca.
64 29.30°S , two records are located between 32° - 34°S and start in the mid-late 1970s, and the
65 remaining record from Tierra del Fuego (54.8°S) starts in 2001. Discontinued, short-term glacier
66 mass balance measurements (see e.g. Popovnin et al. 1999) and recent programs initiated at new
67 sites (e.g. Rivera et al. 2005; Rabatel et al. 2011; Ruiz et al. 2013) complete the network of direct
68 glacier mass balance data currently available in southern South America. Although not optimal in
69 terms of spatial coverage, arguably the single most important limitation of this network is the
70 short period of time covered by consistent, reliable records. Of the two longest mass balance
71 series mentioned above (glaciar Echaurren Norte and glaciar Piloto Este in the Central Andes, see
72 Table 1.1 in WGMS 2013), only the series from Echaurren Norte in Chile (Fig. 1A-C) provides a
73 complete record spanning more than 35 years. In fact, this series constitutes the longest direct
74 glacier mass balance record in the Southern Hemisphere (see Escobar et al. 1995a,b; DGA 2010
75 and WGMS 2013) and is thus a “reference” glacier in the WGMS global assessments. The mass
76 balance record from glaciar Piloto Este (located ca. 100 km to the north in Argentina; Fig. 1A)

77 covers the 1979-2002 period and contains several data gaps that have been interpolated using
78 various techniques (Leiva et al. 2007).

79
80 Many studies dealing with recent climate and glacier changes in southern South America have
81 pointed out the shortness, poor quality, or absence of climatic records at high elevation sites or in
82 the proximity of glaciers in the Andes (Villalba et al. 2003; Rivera et al. 2005; Masiokas et al.
83 2008; Rasmussen et al. 2007; Falvey and Garreaud 2009; Pellicciotti et al. 2014; Vuille et al.
84 2015). Given the lack of suitable data, many climatic assessments have used records from distant,
85 low elevation weather stations and/or gridded datasets to estimate conditions and recent climate
86 variability within the Andean range. It is interesting to note, however, that the amount of hydro-
87 climatic information (in particular from solid and liquid precipitation, and hydrologic variables)
88 is comparatively better for those portions of the southern Andes that support large populated
89 centers and where the water provided by the mountains is vital for human consumption,
90 agriculture, industries and/or hydropower generation. In these areas, mainly between ca. 29° and
91 42°S, local and national water resource agencies have monitored a well-maintained network of
92 hydrologic and meteorological stations for several decades (see e.g. Masiokas et al. 2006, 2010).
93 The data from the stations in this region are slowly becoming publicly available and are
94 substantially better in terms of quantity and quality than those for the less populated, more
95 inaccessible areas in southern Patagonia or in the Desert Andes of northern Chile and Argentina.

96
97 The Central Andes of Chile and Argentina between ~31° and 35°S (see Lliboutry 1998) have a
98 mean elevation of about 3500 m with several peaks reaching over 6000 m (Fig. 1A). The climate
99 of this region is characterized by a Mediterranean regime with a marked precipitation peak during
100 the cold months (April to October) and little precipitation during the warm summer season
101 (November to March; Fig. 1D). Almost all of the moisture comes from westerly Pacific frontal
102 systems, precipitating as rainfall in the Chilean lowlands and as snow in the Andes to the east
103 (Miller 1976; Aceituno 1988; Garreaud 2009). The snow accumulated in the mountains during
104 winter remains frozen until the onset of the melt season (usually October-November), producing
105 a unimodal snowmelt-dominated regime for all rivers originating on either side of the Andes at
106 these latitudes (Masiokas et al. 2006; Cara et al. in press). This relatively simple configuration
107 entails some potential benefits for the study and understanding of the hydro-climatic and

108 glaciological processes in this region: First, the strong co-variability between total rainfall
109 amounts measured in central Chile and winter snow accumulation and river discharges recorded
110 in the Andes (see Fig. 2) allows the use of a relatively limited number of station records to
111 capture the main regional hydro-climatic patterns. The strong common signal among these
112 variables also offers the possibility of inferring or reconstructing selected instrumental data (e.g.
113 winter snow accumulation, which begins in 1951) using data from other well-correlated variables
114 with a longer temporal coverage (e.g. Andean streamflow records which are available since
115 1909). Masiokas et al. (2012) used these relationships to extend Andean snowpack variations
116 using central Chile rainfall records and precipitation-sensitive tree-ring width series.

117
118 In contrast to the well-known similarities between precipitation (solid and liquid) and surface
119 runoff, the spatial and temporal patterns of high-elevation temperature records in the Central
120 Andes of Chile and Argentina are still poorly understood. Falvey and Garreaud (2009) presented
121 a detailed assessment of temperature trends over the 1979-2006 period along the western margin
122 of subtropical South America, reporting a notable contrast between surface cooling (-
123 0.2°C/decade) in coastal stations and a warming trend of ca. +0.25°C/decade in the Andes only
124 100-200 km inland. However, only two land stations were available with long enough records
125 above 2000 m (i.e. El Yeso and Lagunitas stations in Chile at 2475 and 2765 m, respectively), but
126 radiosonde data from the coastal station Quintero (ca. 33°S) showed comparable positive trends
127 for the free-troposphere (Falvey and Garreaud 2009). This lack of high elevation surface
128 temperature data also restricted the recent assessments of Vuille et al. (2015), who focused their
129 elevation-dependent temperature trend analyses on the region north of 18°S because data were
130 too sparse farther south.

131
132 The station El Yeso (33°40'36"S, 70°05'19"W) is located only 10 km south of glacier Echaurren
133 Norte (Fig. 1B). Mean daily and monthly temperature and total precipitation measurements from
134 this station are available since 1962 but contain several months with missing data prior to 1977
135 (temperature) and 1975 (precipitation). Since 1977, both series are practically complete and
136 updated on a regular basis. To our knowledge, in the entire extra-tropical Andes there is no other
137 operational meteorological station with such a long and complete record of temperature and
138 precipitation variations less than a few kilometres from a glacier, which moreover contains the

139 longest ongoing mass balance monitoring program in the Southern Hemisphere. This rare
140 combination of relatively long, complete climate records near a well-studied glacier site clearly
141 highlights the importance of this unique location for varied glaciological and climatological
142 investigations in the southern Andes.

143
144 In this contribution we use seasonal mass balance records from glacier Echaurren Norte plus
145 local and regionally-averaged monthly hydro-climatic data to model and reconstruct annual
146 glacier mass balance changes over the past 105 years. Since only the glacier-wide seasonal and
147 annual mass balance components are available for ECH, one of the main objectives of the study
148 was to explore the suitability of simple mass balance models that require a minimum amount of
149 input data (Marzeion et al. 2012; see also Kaser et al. 2010). Although this simplistic approach
150 provides limited insight into the intricate physical processes involved in this glacier's intra-
151 annual mass balance variations, it may, nonetheless, offer a useful starting point to address some
152 basic (yet still poorly known) questions regarding the glacier's sensitivity to climate variations.
153 We did not consider a data-intensive approach to measure and model the complex daily energy
154 and mass balance variations of this glacier (e.g. Pellicciotti et al. 2014) because of the lack of the
155 high resolution, *in situ* meteorological and glaciological measurements usually required in these
156 type of analyses. Another primary objective was to use the available, well correlated hydrological
157 records from this region (Fig. 2) to extend the ECH annual mass balance record and evaluate the
158 fluctuations of mass balance over a much longer period than that covered by regular glaciological
159 measurements. Comparisons with other shorter mass balance series and with a record of glacier
160 advances in this region suggest the resulting time series contain a discernible regional footprint.
161 Overall, we believe the findings discussed below constitute a substantial improvement in the
162 understanding of the main patterns and forcings of the glacier mass balance changes in this region
163 and provide a useful background for more detailed glacio-climatic assessments and modeling
164 exercises in this portion of the Andes.

165

166 **2 – Data and Methods**

167 **2.1. Glacier mass balance data**

168 Glacier Echaurren Norte (33°33'S, 70°08'W; hereafter ECH) is located within a southwestern
169 oriented cirque ~50 km southeast of Santiago de Chile, in the headwaters of the Maipo river basin

170 (Fig. 1A-C). ECH provides water to Laguna Negra, a natural lake that together with the nearby El
171 Yeso artificial lake constitute crucial water reservoirs for extensive irrigated lands and for the
172 metropolitan Santiago area in Central Chile.

173
174 Mass balance measurements started at this easily accessible glacier in the austral spring of 1975
175 under the auspices of Dirección General de Aguas (DGA), the institution in charge of monitoring
176 and managing water resources in Chile. Summer and winter mass balance data at ECH have been
177 regularly measured until the present by DGA officials, and have been reported in sporadic
178 internal documents and scientific publications (Peña and Narbona 1978; Peña et al. 1995;
179 Escobar et al. 1995, 1997; DGA 2010). These records have also been reported to the WGMS,
180 from where we obtained the 1975-2012 data used in this manuscript (annual mass balance data
181 extend to 2013; see WGMS 2013 and www.wgms.ch). The glacier has thinned in the last decades
182 and presently consists of small remnants of both clean and debris-covered ice (Fig. 1C). Despite
183 this evident ice mass loss, the elevation range of the glacier has not changed much since
184 measurements started in the mid 1970s. According to Peña and Narbona (1978) and Escobar et al.
185 (1995), in the first years of the mass balance program the glacier covered an area of 0.4 km²
186 distributed over a short elevation range between ca. 3650 and 3880 m asl (Fig. 1C). As this is the
187 only area reported for this glacier, in the analyses and results below we use reference-surface
188 mass balance estimates (i.e. the mass balance that would have been observed if the glacier
189 topography had not changed over the study period; see Cogley et al. 2011).

190
191 Mass balance data from glacier Piloto Este (hereafter PIL) from 1979-2002 and shorter time
192 series from small glaciers and glacierets further north in this region are also available from the
193 WGMS database (Leiva et al. 2007; Rabatel et al. 2011; WGMS 2013; see Fig. 1A and Table 1).
194 Here we compare the cumulative annual mass balance records of these glaciers as independent
195 validation measures of the main patterns and temporal trends observed in the measured and
196 modeled mass balance series from ECH.

197

198 **2.2 Minimal glacier mass balance model**

199 A minimal model only requiring monthly temperature and precipitation data (Marzeion et al.
200 2012) was used to estimate the interannual surface mass balance variations of ECH and to

201 explore the relative importance of temperature and precipitation variability on the ECH records.
 202 In their publication, Marzeion et al. (2012) used gridded precipitation and temperature data to
 203 calibrate individual models for 15 glaciers with existing mass balance measurements in the
 204 greater Alpine region. The climate data used here come from El Yeso, a permanent automatic
 205 weather station maintained by DGA and located ca. 10 km to the south and 1200 m lower than
 206 ECH’s snout (Fig. 1B). The data are freely available at the DGA website (www.dga.cl) and
 207 contain practically complete monthly temperature and precipitation records since 1977 (only four
 208 missing months were filled using their long-term means). The mass balance model can be defined
 209 as follows:

$$210$$

$$211 \quad MB = \sum_{i=1}^{12} (\alpha P_i - \mu(\max(0, T_i - T_{melt}))) \quad (1)$$

212
 213 where MB represents the modeled annual specific mass balance of the glacier, P_i are monthly
 214 total precipitation values at the El Yeso station, and α is a scaling parameter introduced to
 215 compensate for the precipitation gradient between the elevation of this station (rounded here to
 216 2500 m) and the front of ECH (fixed at 3700 m in this analysis). T_i represents mean monthly
 217 temperatures at El Yeso extrapolated to the elevation of the glacier front using a constant lapse
 218 rate of $-0.065^{\circ}\text{C}/100\text{ m}$, and T_{melt} is the monthly mean temperature above which melt occurs. As
 219 indicated in Marzeion et al. (2012), the maximum operator ensures that melting occurs only
 220 during months with mean temperatures above T_{melt} . The parameter μ is expressed in mm K^{-1} and
 221 was introduced to translate the monthly temperature records into monthly ablation values at the
 222 glacier. In order to estimate the parameters α and μ and validate the final model, we performed a
 223 “leave-one-out” cross validation procedure (Michaelsen 1987). In this approach, ECH data for
 224 each year between 1977 and 2012 (common period between the El Yeso data and the ECH mass
 225 balance series) were successively excluded and the minimal mass balance model (Eq. 1)
 226 calibrated with the remaining values. At each step the parameters α and μ were first optimized to
 227 minimize the root mean squared error (rmse; Weisberg 1985) of the modeled values, and then
 228 used to estimate the mass balance data omitted that year. This resulted in 36 predicted values
 229 which were compared to the actual annual mass balance observations to compute validation
 230 statistics of model accuracy and error. The exercise showed that the model parameters are

231 relatively time stable: α ranged between 3.9 and 4.1 (mean value used here = 3.9), whereas μ
232 varied between 89.0 and 91.0 mm K⁻¹ (mean value used = 90.1 mm K⁻¹). The mean estimated
233 value of α indicates that accumulation at the glacier is normally about four times larger than the
234 annual precipitation recorded at El Yeso. The mean estimated value for μ is also reasonable and
235 within the range of values reported by Marzeion et al. (2012) for the 15 glaciers with direct
236 measurements in the European Alps (76-156 mm K⁻¹, see their Table 1). Finally, for the sake of
237 simplicity, we prescribed $T_{melt} = 0^{\circ}\text{C}$ as suggested in Marzeion et al. (2012).

238

239 **2.3 Glacier mass balance reconstruction**

240 In addition to modeling the interannual mass balance variations of ECH using the temperature
241 and precipitation data from El Yeso, we also used regionally representative hydroclimatic
242 indicators to extend the observed glacier mass balance record prior to 1975. The use of these
243 indicators (regionally-averaged series of mean annual river discharges; see Masiokas et al. 2006)
244 was supported by visual comparisons and correlation analyses which showed strong, statistically
245 significant positive associations not only with the winter record at ECH, but also with the annual
246 mass balance series of this glacier (Table 2 and Fig. 2). The correlation was also positive but
247 weaker between the summer component at ECH and the regional snowpack and streamflow
248 series.

249

250 The regionally-averaged record of winter snow accumulation is based on eight selected stations
251 located in the Chilean and Argentinean Andes between 30° and 37°S (Fig. 1A and Table 3). The
252 dataset has been updated from the one used by Masiokas et al. (2012) and contains the longest
253 and most complete snowpack records in this region. Prior to computing the regional average, the
254 individual series were expressed as percentages from their 1981-2010 climatology mean values.
255 A similar approach was used to develop a regional record of mean annual (July-June) streamflow
256 variations. This series was calculated using monthly data from 11 gauging stations with the
257 longest and most complete records in this portion of the Andes (Fig. 1A and Table 3). The
258 resulting snowpack and streamflow composite records cover the 1951-2014 and 1909-2013
259 periods, respectively (Fig. 2).

260

261 The glacier mass balance reconstructions are based on simple linear regression models where the
 262 predictand is the 1975-2013 ECH annual mass balance series and the predictors are, alternatively,
 263 the regional 1951-2014 snowpack and 1909-2013 streamflow records depicted in Fig. 2. Given
 264 the relative shortness of the common period between the predictor and predictand series (39
 265 years), the reconstruction models were also developed using a “leave-one-out” cross-validation
 266 procedure (Michaelsen 1987). Here, linear regression models for each year were successively
 267 calibrated on the remaining 38 observations and then used to estimate the predictand’s value for
 268 the year omitted at each step. A simple linear regression model based on the full calibration
 269 dataset (1975-2013) was finally used to reconstruct the mass balance values over the complete
 270 period covered by the regional time series. The goodness of fit between observed and predicted
 271 mass balance values was tested based on the proportion of variance explained by the regression
 272 models and the normality, linear trend, and first- and higher-order autocorrelation of the
 273 regression residuals. The uncertainties in each reconstructed mass balance value in year t ($\epsilon_{reco, t}$)
 274 were calculated integrating the standard error of the regression estimate (se_{regr}) and the standard
 275 error of the mean annual streamflow values used as predictors in the model ($se_{mean, t}$). This latter
 276 error is derived from the standard deviation of the regional record (σ) and increases as the number
 277 of contributing streamflow series (n_t) decreases back in time (see Table 3).

278

$$279 \quad \epsilon_{reco, t} = \sqrt{se_{regr}^2 + se_{mean, t}^2}, \text{ with} \quad (2)$$

280

$$281 \quad se_{mean, t} = \frac{\sigma}{\sqrt{n_t}} \quad (3)$$

282

283 An independent verification of the reconstructed mass balance records was undertaken by
 284 comparing the cumulative patterns of these series with the cumulative mass balances reported for
 285 glacier Piloto Este and for other glaciers with shorter mass balance series available in this portion
 286 of the Andes (Fig. 1A and Table 1). We also compared the ECH cumulative series (observed and
 287 predicted) with a regional record of glacier advances identified during the 20th century in the
 288 Andes between 29° and 35°S. The latter record was compiled in a recent review of glacier
 289 fluctuations in extratropical South America and is based on direct observations, reports from
 290 documentary evidence, and analyses of aerial photographs and satellite images from this region

291 (see Masiokas et al. 2009). The uncertainty of the cumulative series modeled for ECH ($\epsilon_{cum, t}$)
292 were calculated by propagating (adding) the individual errors estimated for each reconstructed
293 value. That is

$$295 \quad \epsilon_{cum,t} = \sqrt{\epsilon_{reco,t}^2 + \epsilon_{reco,t+1}^2} \quad (4)$$

296

297 **3 – Results**

298 **3.1. Minimal glacier mass balance model**

299 The 1975-2012 winter and summer values observed at ECH are depicted in Fig. 3A. The winter
300 series shows a long term mean of 2.54 m w.eq. and a larger range of variability (std. dev. 1.24 m
301 w.eq.) than the summer series, which fluctuates around a long term mean of -2.93 m w.eq (std.
302 dev. 0.72 m w.eq.). The observed and modeled annual mass balance series are remarkably similar
303 (Fig. 3B) and show a strong positive correlation ($r = 0.883$, $rmse = 0.77$ m w.eq.), indicating that
304 78% of the variance in the ECH record can be accounted for by the minimal model presented in
305 Eq. (1). Both series show similar, slightly negative linear trends and negative means (-0.35 and -
306 0.34 m w.eq. for the observed and modeled series, respectively) over the 1977-2012 interval.

307

308 **3.2. Attribution assessments**

309 In order to test which climate variable (temperature or precipitation) has a stronger influence on
310 the annual mass balance variations at ECH, the glacier mass balance model was also run
311 replacing alternatively the temperature and the precipitation monthly data by their long-term
312 average values. The results from this analysis (Fig. 3C) suggest that precipitation variations
313 constitute the dominant forcing modulating annual glacier mass balance at this site. Regardless of
314 their different absolute values, the precipitation-driven estimates (blue dashed line in Fig. 3C)
315 show a strong positive correlation ($r = 0.882$) and remarkable similarities with the ECH annual
316 mass balance series (red line). In contrast, the temperature-driven estimates (dark red dashed line)
317 show a poorer correlation with the ECH record ($r = 0.240$) and a substantially lower inter-annual
318 variability which only barely follows the variations in the annual mass balance series.

319

320 **3.3 Annual mass balance reconstruction 1909-2013**

321 Fig. 4A shows the reconstruction of the ECH annual mass balance series based on the regional
322 record of mean annual streamflows. The snowpack-based mass balance reconstruction is not
323 shown as it is significantly shorter than the streamflow-based series and shows virtually the same
324 variations over their overlapping interval. The streamflow-based regression model (Table 4) is
325 able to explain 68% of the variance in the annual mass balance series over the 1975-2013 period
326 and shows no apparent sign of model misspecification, offering the possibility of reliably
327 extending the information on glacier mass balance changes back to 1909. This reconstructed
328 mass balance record is almost three times longer than the mass balance record currently available
329 at ECH and shows a strong year-to-year variability embedded within several periods of overall
330 positive or negative conditions (Fig. 4A). In particular, positive mass balance conditions were
331 reconstructed between 1914 and 1941, in the 1980s, and in the late 1990s – early 21st century. In
332 contrast, the clearest sustained period of negative mass balances occurred between the 1940s and
333 the 1970s.

334
335 The cumulative values of the streamflow-based mass balance reconstruction show a very good
336 correspondence with the observed cumulative series and an overall negative trend between 1909
337 and 2013 (Fig. 4B). Within this century-long negative trend, a prominent period of extended
338 positive mass balances can be observed between the mid 1910s and the early 1940s. The peak of
339 this extended positive period occurred in the early 1920s and reached almost 10 m w.eq. above
340 the 1909 mass balance starting value. After 1941 and during the following four decades the
341 cumulative mass balance series shows an impressive decline that is interrupted in 1980 by a ~10-
342 year long period of sustained positive conditions (Fig. 4B). Since the early 1990s and until 2013
343 the cumulative mass balance series resumes the negative tendency, only interrupted by a short-
344 lived period of positive conditions in the first years of the 21st century. It is important to note,
345 however, that ascribing absolute values to this reconstructed cumulative series is complicated and
346 should be used with caution due to the large uncertainties involved, and the fact that we are using
347 reference-surface mass balance estimates (Cogley et al. 2011). Between 1975 and 2013 the lower
348 elevation of the glacier did not change much (see Fig. 1C) and therefore the reference-surface and
349 the conventional mass balance estimates are probably roughly equivalent. However, for earlier
350 decades and without historical information on the glacier area and frontal position, it is difficult
351 to estimate the impacts of changing glacier geometry on the actual mass balance of this glacier.

352

353 **3.4 Comparison with other glacier records**

354 Examination of the main patterns in the reconstructed cumulative mass balance series shows a
355 good correspondence with a regional record of glacier advances identified in the Central Andes
356 over the past 100 years (Masiokas et al. 2009; Fig. 4C). In most cases, the glacier advances are
357 concentrated during, or soon after, the periods of sustained positive mass balances reconstructed
358 or observed at ECH. This situation is particularly clear in the 1980s and 1990s, where a large
359 number of glacier advances were identified during and/or immediately after the peak in mass
360 balances that culminated in 1989 (Fig. 4BC). Glacier advances were also identified in the 1930s,
361 1940s and 1950s likely associated with the extended period of cumulative positive mass balances
362 that culminated in the early 1940s. A few well documented advances identified in this region
363 between 2003 and 2007 may be associated with the minor peak in cumulated mass balances
364 observed at the turn of the 21st century (Fig. 4BC).

365

366 The cumulative variations in the modeled and observed mass balance series from ECH are also
367 very similar to those observed in the 1979-2002 cumulative record of PIL, providing additional
368 support for the overall reliability of the reconstructed time series (Fig. 5). The cumulative
369 tendency of PIL appears to be “smoother” than the ECH series, but still shows slightly positive or
370 near equilibrium conditions between the late 1970s and the mid 1980s followed by a sharp
371 decline until the turn of the 21st century. The cumulative series from other glaciers located further
372 north in the Pascua Lama and Cordillera de Colanguil areas (Fig. 1A and Table 1) only cover the
373 last decade or so of the ECH record. However, in all cases their overall tendency is similar and
374 markedly negative, reflecting the sustained unfavorable conditions that these ice masses have
375 endured in recent years. It is interesting to note that the smaller glaciers (Table 1 and Fig. 5) are
376 the ones consistently showing the steepest negative cumulative trends whereas the largest glacier
377 (glaciar Guanaco, with ca. 1.8 km² in 2007) shows the least negative trend.

378

379 **4 – Discussion and Conclusions**

380 Compared to other mountainous glacierized areas, the extratropical Andes in southern South
381 America contain one of the least complete networks of *in situ* glacier mass balance and high-
382 elevation climate records in the world. This scarcity of basic information in this extensive and

383 glaciologically diverse region has been highlighted on many occasions, and several recent studies
384 have attempted to overcome this limitation by estimating mass balance changes through remote
385 sensing and/or modeling approaches of varied complexity and spatial coverage (e.g. Casassa et
386 al. 2006; Radić et al. 2013; Lenaerts et al. 2014; Pellicciotti et al. 2014; Schaeffer et al. 2013,
387 2015). With such limited data availability, the few existing glacier mass balance records become
388 particularly relevant as they provide crucial information and validation measures for many
389 glaciological, climatological and hydrological analyses.

390
391 In this paper we analyzed an up-to-date compilation of the longest and most complete *in situ*
392 glacier mass balance and hydro-climatic records from the Andes between 29° and 37°S to address
393 some basic (yet poorly known) glaciological issues in this region. First, we show that it is
394 possible to estimate annual glacier mass balance changes using very simple modeling approaches.
395 Results from a minimal model requiring only monthly temperature and precipitation data (eq. 1)
396 revealed that up to 78% of the variance in the annual mass balance series between 1977 and 2012
397 could be captured simply using available records from the El Yeso station, ca. 10 km from the
398 glacier (Fig. 1A and 3B). Winter precipitation variability appears to be the dominant forcing
399 modulating annual mass balances at ECH, with temperature variations likely playing a secondary
400 role (Fig. 3C). This is particularly interesting because it contrasts with the findings in other
401 regions where the recent glacier behavior is generally more strongly related to changes in
402 temperature instead of precipitation (e.g. Marzeion et al. 2012). However, and although Peña and
403 Narbona (1978) also noted a dominant influence of the winter accumulation term on the resulting
404 annual mass balance of this glacier, the results should be assessed with caution given the
405 simplistic nature of our model and the various factors that ultimately affect the annual mass
406 balance at this site. For example, more detailed assessments should also consider the impact of
407 sublimation on the mass balance of glaciers in this high arid portion of the Andes (McDonnell et
408 al. 2013; Pellicciotti et al. 2014).

409
410 To test the reliability of the temperature records used to model the glacier mass balance series we
411 correlated the El Yeso monthly temperature record with ERA Interim gridded reanalysis
412 temperatures for the 700 mb geopotential height (roughly 3000 m asl), and also with a 0°C
413 isotherm elevation series available from central Chile (Fig. 6). The El Yeso temperature record

414 shows strong positive correlations with ERA Interim gridded data over an extensive region that
415 includes central Argentina, central Chile and an adjacent area in the Pacific Ocean (Fig. 6A). The
416 El Yeso temperature record also shows clear similarities and a positive significant correlation
417 with the 0°C isotherm elevation series over the 1977-2004 interval (Fig. 6B-C). The
418 independence of these three datasets indicates that the El Yeso mean monthly temperature data
419 are reliable and that the poor performance of this variable in the mass balance modeling exercise
420 is not related to the overall quality of the temperature series. Although this issue is beyond the
421 main purposes of this study, more complex modeling approaches are also needed to evaluate if
422 climate data at higher temporal resolution (instead of monthly values as used here) are capable of
423 capturing a larger percentage of the mass balance variations observed at ECH.

424
425 Annual mass balance variations observed at ECH can also be reproduced or estimated accurately
426 through simple linear regression using regionally-averaged winter snowpack or annual
427 streamflow records as predictors (Fig. 4A). This is due to the existence of a strong common
428 hydroclimatic signal in this region, which results in very similar inter-annual variations in winter
429 snow accumulation, mean annual river discharges, and glacier mass balance changes such as
430 those measured at ECH (Fig. 2). This simple approach allows extending the information on
431 glacier mass balance changes several decades prior to the beginning of in situ measurements
432 (back to 1909), and offers the opportunity of putting the existing glacier record in a longer term
433 perspective. Many of the extreme values reconstructed in this study have been documented in
434 historical reports and recent analyses of instrumental hydro-climatic data. For example, the
435 extreme positive values of 1914 and 1919 coincide with extremely wet winters in central Chile
436 (see e.g. Fig. 2; Taulis 1934; Masiokas et al. 2012), whereas the period with above average
437 balances centered in the 1980s or the negative conditions between the 1940s and 1970s have been
438 identified, respectively, as the snowiest and driest intervals during the instrumental era in this
439 region (Masiokas et al. 2010). Examination of the main intra- to multi-decadal patterns in this
440 extended series also indicates that the sustained negative mass balance conditions reported for
441 ECH in recent years are not unusual and were probably surpassed by more negative and longer
442 periods between the 1940s and 1970s (Fig. 4A). However, the impact of a few consecutive years
443 of negative mass balances are more serious today than several decades ago because of the low
444 volume of ice remaining and the poorer overall “health” of the glacier.

445
446 The cumulative series of the reconstructed mass balances values (Fig. 4B) shows a steep negative
447 trend that is consistent with the recent loss of ice reported for other glaciers in this region (Fig. 5;
448 Escobar et al. 1995; Rivera et al. 2000; Masiokas et al. 2009). This negative trend has been
449 temporarily interrupted by periods of sustained positive mass balances that, in most cases,
450 precede or coincide with recent glacier re-advances identified at these latitudes in the Andes
451 (Masiokas et al. 2009; Fig. 4C). The clearest example is the relationship between the peak in
452 cumulative mass balances in the mid-late 1980s and the 11 documented glacier advances in the
453 following decade. It is also interesting to note that several of the glacier events that occurred after
454 periods of positive mass balances have been identified as surges (Helbling 1935; Espizua 1986;
455 Masiokas et al. 2009; Pitte et al. in review). The well-known surges of Grande del Nevado glacier
456 (in the Plomo massif area) in 1933-34, 1984-85, and 2004-2007 are particularly noteworthy as
457 they consistently occurred near the culmination of the three periods with overall positive mass
458 balances in the 1920s-30s, in the 1980s and in the first decade of the 21st century (Fig. 4B). In
459 agreement with the progressively smaller magnitude of these peaks in the cumulative mass
460 balance series, the three Grande del Nevado surges also showed a decreasing power and
461 transferred progressively smaller quantities of mass from the upper to the lower parts of the
462 glacier. Two recent surges of Horcones Inferior glacier in the nearby Mt. Aconcagua area also
463 occurred in the mid 1980s and again between 2002 and 2006, suggesting a possible connection
464 between the development of surging events and the periods with overall positive mass balance
465 conditions in this region (Pitte et al. in review).

466
467 The fact that only limited information is available for ECH together with the use of reference-
468 surface mass balance estimates (see section 2.1) pose interesting yet complicated questions
469 regarding the applicability of this series in related glaciological and/or climatological
470 assessments. Since reference-surface mass balance variations are more closely related to changes
471 in climate than the conventional mass balance of a glacier (Cogley et al. 2011), the reconstructed
472 series discussed here is arguably more relevant to climate-change related studies rather than
473 hydrological studies. If the purpose is to evaluate the hydrological contribution of this ice mass
474 over the last century, then conventional mass balance estimates are necessarily required to take
475 the changing glacier geometry into account. In any case, and considering the relevance of the

476 observed ECH series for regional, hemispheric and global mass balance studies, a reanalysis
477 (Zemp et al. 2011) of the entire mass balance record would probably produce important
478 worthwhile information to properly assess the hydrological impact of the recent ice mass losses
479 in this semi-arid region (e.g. Ragetli et al. 2014). This issue is particularly relevant due to the
480 extended droughts experienced in recent years and the increasing socio-economic conflicts over
481 the limited water resources (almost entirely originating in the mountains) arising on both sides of
482 the Andes.

483
484 Keeping these caveats in mind, the common pattern of strongly negative mass balances, the
485 similarities with the few available glacier chronologies, and the regional nature of the predictors
486 used in the ECH reconstruction suggest that this series may nonetheless be considered
487 representative (in relative terms) of the mass balance changes during recent decades in other less
488 studied areas in this region. Reliable data from a larger number of glaciers together with
489 additional studies of the glacier-climate relationships are, however, still needed to support this
490 hypothesis and to identify, for example, the main climatic forcings behind the recent glacier
491 shrinkage observed in the Central Andes of Chile and Argentina (Masiokas et al. 2009). This is a
492 challenging issue due to several factors, including the serious lack of glacier mass balance series
493 and high-elevation climate records, the complex dynamic response of individual glaciers to
494 similar changes in climate, and the great variety of glaciers existing in this region (Pellicciotti et
495 al. 2014). The results discussed in this study offer a useful starting point to address the various
496 pending issues mentioned above and will hopefully stimulate further glaciological, climatological
497 and hydrological research in this poorly known mountainous region.

498

499 **6 – Acknowledgements**

500 This work was funded by Consejo Nacional de Investigaciones Científicas y Técnicas
501 (CONICET, Argentina), FONDECYT Grant 1121106, and FONDAP Grant 15110009 (Chile).
502 We greatly acknowledge the World Glacier Monitoring Service (<http://www.wgms.ch>),
503 Dirección General de Aguas (<http://www.dga.cl>), Dirección Meteorológica de Chile
504 (<http://www.meteochile.gob.cl>), and Subsecretaría de Recursos Hídricos
505 (<http://www.hidricosargentina.gov.ar>) for providing the data used in this study. ERA-Interim
506 reanalysis data and correlation maps were provided by the freely available Climate Explorer

507 online application maintained by Geert Jan van Oldenborgh at the Royal Netherlands
508 Meteorological Institute (KNMI; <http://climexp.knmi.nl/>). E. Berthier acknowledges support
509 from the French Space Agency (CNES) through his TOSCA program.

510 **7 – References**

- 511
- 512 Aceituno, P. (1988), On the functioning of the Southern Oscillation in the South American sector.
513 Part I: Surface climate, *Mon. Weather Rev.*, 116, 505– 524.
- 514 Casassa, G., Rivera, A. and Schwikowski, M. 2006. Glacier mass-balance data for southern South
515 America (30°S-56°S). In: *Glacier Science and Environmental Change* (ed P. G. Knight),
516 Blackwell Publishing, Malden, MA, USA. doi: 10.1002/9780470750636.ch47
- 517 Cara, L., Masiokas, M. Viale, R. Villalba (in press). Assessing snow cover variations in the
518 Río Mendoza upper basin using MODIS satellite imagery. *Revista Meteorológica*, 25 p.
519 (in Spanish).
- 520 Cogley, J.G., R. Hock, L.A. Rasmussen, A.A. Arendt, A. Bauder, R.J. Braithwaite, P. Jansson, G.
521 Kaser, M. Möller, L. Nicholson and M. Zemp, 2011, *Glossary of Glacier Mass Balance*
522 *and Related Terms*, IHP-VII Technical Documents in Hydrology No. 86, IACS
523 Contribution No. 2, UNESCO-IHP, Paris.
- 524 DGA. 2009. Radio Eco-sondaje en la cuenca del río Maipo y mediciones glaciológicas en el
525 glaciar Tyndall, Campo de Hielo Sur. Dirección General de Aguas, Santiago de Chile,
526 S.I.T. 204, 95 pp.
- 527 DGA, 2010. Balance de masa en el glaciar Echaurren Norte temporadas 1997-1998 a 2008-2009.
528 Dirección General de Aguas, Santiago de Chile, 32 pp.
- 529 Escobar, F., Casassa G, Pozo V. 1995a. Variaciones de un glaciar de montaña en los Andes de
530 Chile central en las últimas dos décadas. *Bull Inst Fr Etud Andin* 1995;24(3):683–95.
- 531 Escobar, F., Pozo, V., Salazar, A., y Oyarzo, M., 1995b. Balance de masa en el glaciar Echaurren
532 Norte, 1975 a 1992. Resultados preliminares. Dirección General de Aguas. (Publicación
533 DGA, H.A. y G. 95/1), 106 p.
- 534 Escobar, F. and Garín, C. 1997. Complemento N° 1, años 1993-1996, al “Balance de masa en el
535 glaciar Echaurren Norte, 1975 a 1992. Resultados preliminares”. Dirección General de
536 Aguas. (Publicación DGA, H.A. y G. 97/1), 18 p.
- 537 Espizua, L. 1986. Fluctuations of the Río del Plomo Glaciers. *Geografiska Annaler*, 68A(4): 317-
538 327.
- 539 Falvey, M.; Garreaud, R.D. 2009. Regional cooling in a warming world: Recent temperature
540 trends in the southeast Pacific and along the west coast of subtropical South America

541 (1979–2006). *Journal of Geophysical Research* 114, D04102,
542 doi:10.1029/2008JD010519.

543 Garreaud, R.D. 2009. The Andes climate and weather. *Advances in Geosciences* 7, 1–9.

544 Helbling, R. 1935. The origin of the Río Plomo ice-dam. *The Geographical Journal*, 8(1): 41-49.

545 Kaser, G., Grosshauser, M., and Marzeion, B.: Contribution potential of glaciers to water
546 availability in different climate regimes, *P. Natl. Acad. Sci. USA*, 107, 20223–20227,
547 doi:10.1073/pnas.1008162107, 2010.

548 Le Quesne, C., et al. (2009), Long-term glacier variations in the Central Andes of Argentina and
549 Chile, inferred from historical records and tree-ring reconstructed precipitation,
550 *Palaeogeogr. Palaeoclimatol. Palaeoecol.*, 281, 334-344.

551 Leiva, J.C.; Cabrera, G.A.; Lenzano, L.E. 2007. 20 years of mass balances on the Piloto glacier,
552 Las Cuevas river basin, Mendoza, Argentina. *Global and Planetary Change* 59, 10–16.

553 Lenaerts, J.T.M., M.R. van den Broeke, J.M. van Wessem, W.J. van de Berg, E. van Meijgaard,
554 L.H. van Ulft, and M. Schaefer. 2014. Extreme precipitation and climate gradients in
555 Patagonia revealed by high-resolution regional atmospheric climate modeling. *Journal of*
556 *Climate* 27, 4607–4621.

557 Lliboutry, L., 1998: *Glaciers of the dry Andes. Satellite Image Atlas of Glaciers of the World:*
558 *South America*, R. S. Williams and J. G. Ferrigno, Eds., USGS Professional Paper 1386-I.
559 Available online at <http://pubs.usgs.gov/prof/p1386i/index.html>.

560 MacDonell, S., C. Kinnard, T. Mölg, L. Nicholson, and J. Abermann. 2013. Meteorological
561 drivers of ablation processes on a cold glacier in the semi-arid Andes of Chile. *The*
562 *Cryosphere*, 7, 1513–1526, doi:10.5194/tc-7-1513-2013

563

564 Marzeion, B., M. Hofer, A. H. Jarosch, G. Kaser, and T. Molg. 2012. A minimal model for
565 reconstructing interannual mass balance variability of glaciers in the European Alps. *The*
566 *Cryosphere*, 6, 71–84, doi:10.5194/tc-6-71-2012.

567 Masiokas, M.H.; Villalba, R.; Luckman, B.; LeQuesne, C.; Aravena, J.C. 2006. Snowpack
568 variations in the central Andes of Argentina and Chile, 1951-2005: Large-scale
569 atmospheric influences and implications for water resources in the region. *Journal of*
570 *Climate* 19 (24), 6334-6352.

571 Masiokas, M.H.; Villalba, R.; Luckman, B.; Delgado, S.; Lascano, M.; Stepanek, P. 2008. 20th-
572 century glacier recession and regional hydroclimatic changes in northwestern Patagonia.
573 *Global and Planetary Change* 60 (1-2), 85-100.

574 Masiokas, M.H.; Rivera, A.; Espizua, L.E.; Villalba, R.; Delgado, S.; Aravena, J.C. 2009. Glacier
575 fluctuations in extratropical South America during the past 1000 years. *Palaeogeography,*
576 *Palaeoclimatology, Palaeoecology* 281 (3-4), 242-268.

577 Masiokas, M.H.; Villalba, R.; Luckman, B.H.; Mauget, S. 2010. Intra- to multidecadal variations
578 of snowpack and streamflow records in the Andes of Chile and Argentina between 30°
579 and 37°S. *Journal of Hydrometeorology* 11 (3), 822-831.

580 Masiokas, M.H.; Villalba, R.; Christie, D.A.; Betman, E.; Luckman, B.H.; Le Quesne, C.; Prieto,
581 M.R.; Mauget, S. 2012. Snowpack variations since AD 1150 in the Andes of Chile and
582 Argentina (30°-37°S) inferred from rainfall, tree-ring and documentary records. *Journal of*
583 *Geophysical Research - Atmospheres*, 117, D05112, doi:10.1029/2011JD016748.

584 Miller, A., 1976: The climate of Chile. *World Survey of Climatology*. W. Schwerdtfeger, Ed.,
585 Vol. 12, Elsevier, 113–218.

586 Pellicciotti, F.; Ragetti, S.; Carenzo, M.; McPhee, J. 2014. Changes of glaciers in the Andes of
587 Chile and priorities for future work. *Science of the Total Environment* 493, 1197–1210.

588 Peña, H.; Narbona, J. 1978. Proyecto Glaciar Echaurren Norte, Informe preliminar. Dirección
589 General de Aguas, Departamento de Hidrología (in Spanish). 75 p.

590 Popovnin, V.V., Danilova, T.A., Petrakov, D.A., 1999. A pioneer mass balance estimate for a
591 Patagonian glacier: Glaciar De los Tres, Argentina. *Global and Planetary Change* 22 (1),
592 255–267.

593 Rabatel, A.; H. Catebrunet, V. Favier, L. Nicholson, C. Kinnard. 2011. Glacier changes in the
594 Pascua Lama region, Chilean Andes (29 S): recent mass balance and 50 years surface area
595 variations. *The Cryosphere* 5, 1029–1041.

596 Radić, V.; Bliss, A.; Beedlow, A.C.; Hock, R.; Miles, E.; Cogley, J.G.; Regional and global
597 projections of twenty-first century glacier mass changes in response to climate scenarios
598 from global climate models. *Climate Dynamics*, DOI 10.1007/s00382-013-1719-7

599 Ragetti S., Cortés G., McPhee J., Pellicciotti F. 2014. An evaluation of approaches for modelling
600 hydrological processes in high-elevation, glacierized Andean watersheds, *Hydrological*
601 *Processes* 28, 5674–5695, doi: 10.1002/hyp.10055

602 Rignot, E., A. Rivera, G. Cassasa. 2003. Contribution of the Patagonia Icefields to sea level rise.
603 Science 302, 434-437.

604 Rasmussen, L., Conway, H., Raymond, C., 2007. Influence of upper air conditions on the
605 Patagonia Icefields. *Global and Planetary Change* 59, 203–216.

606 Rivera, A., G. Casassa, C. Acuña, and H. Lange, 2000: Recent glacier variations in Chile (in
607 Spanish). *Investigaciones Geográficas* 34, 29–60.

608 Rivera, A.; Bown, F; Casassa, G.; Acuña, C.; Clavero, J. 2005. Glacier shrinkage and negative
609 mass balance in the Chilean Lake District (40°S). *Hydrological Sciences Journal*, 50(6):
610 963-974.

611 Ruiz, L.; Pitte, P.; Masiokas, M. 2013. The initiation of mass balance studies on the Argentinean
612 glaciers on Mount Tronador. CRN2047 Science Meeting, Uspallata, Argentina, April 21-
613 25, 2013.

614 Schaefer, M., Machguth, H., Falvey, M., Casassa, G. 2013. Modeling past and future surface
615 mass balance of the Northern Patagonia Icefield. *J. Geophys. Res.*, 118, 571–588, doi:
616 10.1002/jgrf.20038.

617 Schaefer M., Machguth H., Falvey M., Casassa G., Rignot E. 2015. Quantifying mass balance
618 processes on the Southern Patagonia Icefield. *Cryosphere*, 9(1), 25–35, doi: 10.5194/tc-9-
619 25-2015.

620 Taulis, E. 1934. De la distribucion de pluies au Chili. *Matér. Étude Calamités*, 33, 3-20.

621 Villalba, R.; Lara, A.; Boninsegna, J.A.; Masiokas, M.H.; Delgado, S.; Aravena, J.C.; Roig, F.;
622 Schmelter, A.; Wolodarsky, A.; Ripalta, A. 2003. Large-scale temperature changes across
623 the southern Andes: 20th-century variations in the context of the past 400 years. *Climatic*
624 *Change* 59 (1-2), 177-232.

625 WGMS. 2013. Glacier Mass Balance Bulletin No. 12 (2010-2011). Zemp, M., Nussbaumer, S.U.,
626 Naegeli, K., Gärtner-Roer, I., Paul, F., Hoelzle, M., and Haeberli, W. (eds.), ICSU (WDS)
627 / IUGG (IACS) / UNEP / UNESCO / WMO, World Glacier Monitoring Service, Zurich,
628 Switzerland: 106 pp., publication based on database version: doi: 10.5904/wgms-fog-
629 2013-11.

630 Zemp, M., E. Thibert, M. Huss, D. Stumm, C. Rolstad Denby, C. Nuth, S.U. Nussbaumer, G.
631 Moholdt, A. Mercer, C. Mayer, P. C. Joerg, P. Jansson, B. Hynek, A. Fischer, H. Escher-

632 Vetter, H. Elvehøy, and L. M. Andreassen. 2013. Reanalysing glacier mass balance
633 measurement series. *The Cryosphere*, 7, 1227–1245, doi:10.5194/tc-7-1227-2013
634

635 **Table 1.** Basic information of the glacier mass balance series used in this study. (*) Country: CL:
 636 Chile; AR: Argentina.

Name	ID in Fig. 1	Lat., Long.	Area in km² (year)	Period	Ctry*	References
Echaurren Norte	ECH	33°33'S, 70°08'W	0.226 (2008)	1975-2013	CL	DGA 2009; Barcaza (DGA); WGMS 2013
Piloto Este	PIL	32°13'S, 70°03'W	0.504 (2007)	1979-2002	AR	Leiva et al. 2007; WGMS 2013
Conconta Norte	COL	29°58'S, 69°39'W	0.089 (2012)	2008-2013	AR	Cabrera and Leiva (IANIGLA); WGMS 2013
Brown Superior	COL	29°59'S, 69°38'W	0.191 (2012)	2008-2013	AR	Cabrera and Leiva (IANIGLA); WGMS 2013
Los Amarillos	COL	29°18'S, 69°59'W	0.954 (2012)	2008-2013	AR	Cabrera and Leiva (IANIGLA); WGMS 2013
Amarillo	PAS	29°18'S, 70°00'W	0.243 (2012)	2008-2013	CL	Cabrera and Leiva (IANIGLA); WGMS 2013
Toro 1	PAS	29°20'S, 70°01'W	0.071 (2007)	2004-2009	CL	Rabatel et al. 2011; WGMS 2013
Toro 2	PAS	29°20'S, 70°01'W	0.066 (2007)	2004-2009	CL	Rabatel et al. 2011; WGMS 2013
Esperanza	PAS	29°20'S, 70°02'W	0.041 (2007)	2004-2009	CL	Rabatel et al. 2011; WGMS 2013
Guanaco	PAS	29°19'S, 70°00'W	1.836 (2007)	2004-2013	CL/ AR	Rabatel et al. 2011; Rivera (CECs); WGMS 2013

637

638 **Table 2.** Correlation analyses between the ECH mass balance series and regional hydro-climatic
 639 records. The number of observations used in each correlation test is indicated in parenthesis.
 640 Note: * (**) Pearson correlation coefficient is significant at the 95% (99%) confidence level.
 641

	Winter ECH	Annual mass balance ECH	Regional snowpack	Regional streamflow
Summer ECH	0.245 (38)	0.648** (38)	0.447** (38)	0.395* (38)
Winter ECH		0.897** (38)	0.796** (38)	0.834** (38)
Annual mass balance ECH			0.829** (39)	0.826** (39)
Regional snowpack				0.916** (63)

642
 643

644 **Table 3.** Stations used to develop regionally-averaged series of mean annual river discharges and
645 winter maximum snow accumulation for the Andes between 30° and 37°S. Mean annual
646 streamflow values refer to a July-June water year. Note: (*) The 1981-2010 climatology values
647 for each station are expressed as mm w.eq. for snowpack and as m³ s⁻¹ for streamflow. In the case
648 of the San Juan and Cachapoal rivers, the mean values used correspond to the 1981-2007 and
649 1981-2001 periods, respectively. Data sources: (DGA) Dirección General de Aguas, Chile; (DGI)
650 Departamento General de Irrigación, Mendoza, Argentina; (SSRH) Subsecretaría de Recursos
651 Hídricos, Argentina. See Masiokas et al. (2013) for further details.
652

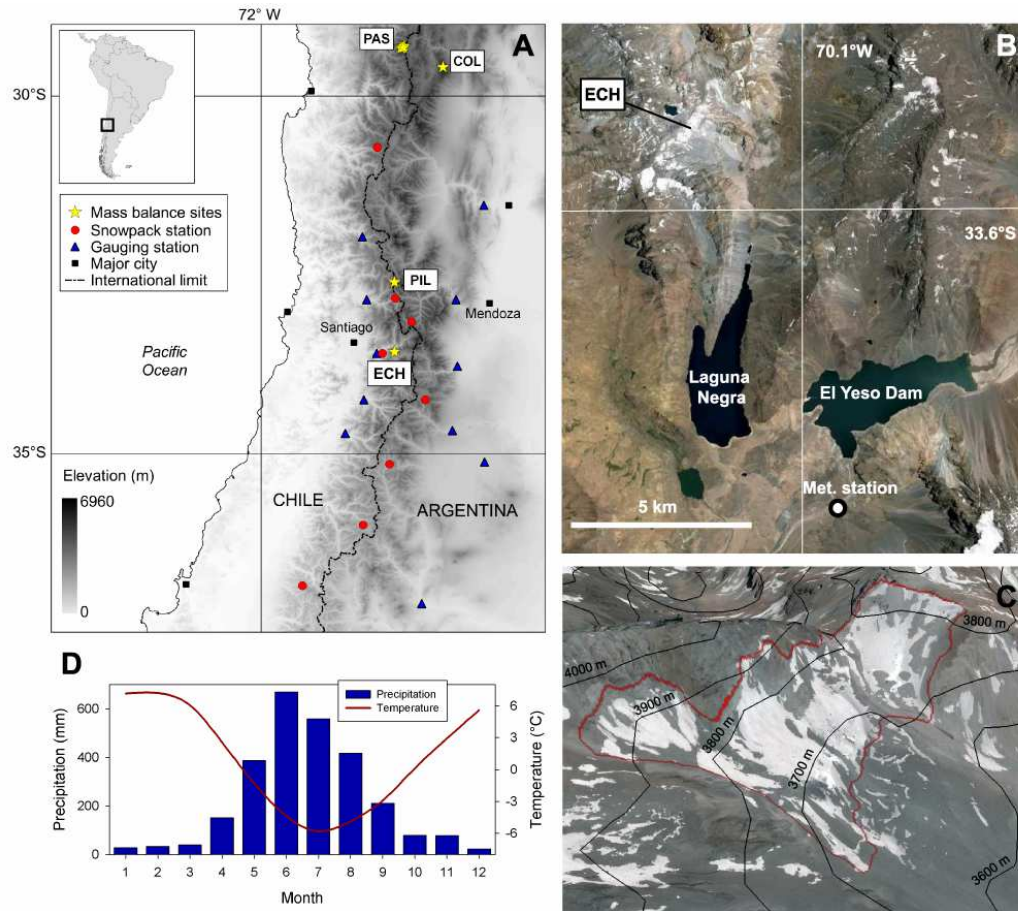
Variable	Station	Lat., Long.	Elev.	Period	1981-2010 mean*	Data source
A - Snowpack	Quebrada Larga	30°43'S, 70°22'W	3500 m	1956-2014	273	DGA
	Portillo	32°50'S, 70°07'W	3000 m	1951-2014	703	DGA
	Toscas	33°10'S, 69°53'W	3000 m	1951-2014	354	DGI
	Laguna Negra	33°40'S, 70°08'W	2768 m	1965-2014	632	DGA
	Laguna del Diamante	34°15'S, 69°42'W	3310 m	1956-2014	472	DGI
	Valle Hermoso	35°09'S, 70°12'W	2275 m	1952-2014	756	DGI
	Lo Aguirre	36°00'S, 70°34'W	2000 m	1954-2014	934	DGA
	Volcán Chillán	36°50'S, 71°25'W	2400 m	1966-2014	757	DGA
B - Streamflow (river)	Km. 47.3 (San Juan)	31°32'S 68°53'W	945 m	1909- 2007	68.2	SSRH
	Guido (Mendoza)	32°51'S 69°16'W	1550 m	1909-2013	52.4	SSRH
	Valle de Uco (Tunuyán)	33°47'S 69°15'W	1200 m	1954-2013	30.6	SSRH
	La Jaula (Diamante)	34°40'S 69°19'W	1500 m	1938-2013	35.6	SSRH
	La Angostura (Atuel)	35°06'S 68°52'W	1200 m	1948-2013	39.1	SSRH
	Buta Ranquil (Colorado)	37°05'S 69°44'W	850 m	1940-2013	154.8	SSRH
	Cuncumén (Choapa)	31°58'S 70°35'W	955 m	1941-2013	10.3	DGA
	Chacabuquito (Aconcagua)	32°51'S 70°31'W	1030 m	1914-2013	34.7	DGA
	El Manzano (Maipo)	33°36'S 70°23'W	890 m	1947-2013	123.0	DGA
	Termas de Cauquenes (Cachapoal)	34°15'S 70°34'W	700 m	1941-2001	93.6	DGA
	Bajo Los Briones (Tinguiririca)	34°43'S 70°49'W	518 m	1942-2013	53.8	DGA

653

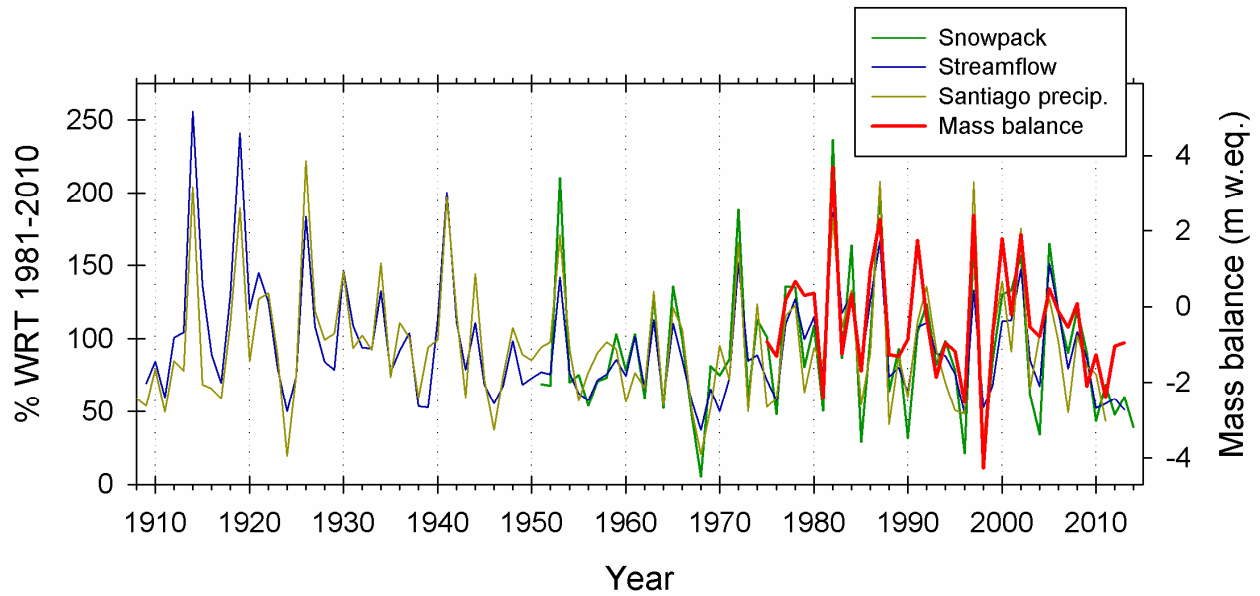
654 **Table 4.** Summary statistics for the simple linear regression models used to estimate ECH annual
655 mass balances using regional snowpack and streamflow records. Notes: (adj r^2) adjusted
656 coefficient of determination used to estimate the proportion of variance explained by regression;
657 (F) F-ratio for ANOVA test of the null hypothesis that all model coefficients are 0; (Se) standard
658 error of the estimate; (rmse) root-mean-squared error of regression. (b0) constant of regression
659 model; (b1) regression coefficient; (DWd) Durbin-Watson d statistic used to test for first-order
660 autocorrelation of the regression residuals. (Port. Q) Portmanteau Q statistic to test if high-order
661 autocorrelation in the regression residuals is different from 0. (ns) results are not statistically
662 significant at the 95% confidence level; (**) statistically significant at the 99% confidence level.
663

Predictor	Model statistics						Residual statistics		
	Adj r^2	F	Se	rmse	b0 (std. error)	b1 (std. error)	Slope	DWd	Port. Q
Snowpack	0.686	80.99**	0.889	0.911	-2.899 (0.316)**	0.026 (0.003)**	-0.003ns	2.2ns	5.7ns
Streamflow	0.682	79.49**	0.894	0.919	-4.045 (0.439)**	0.038 (0.004)**	0.006ns	2.3ns	4.9ns

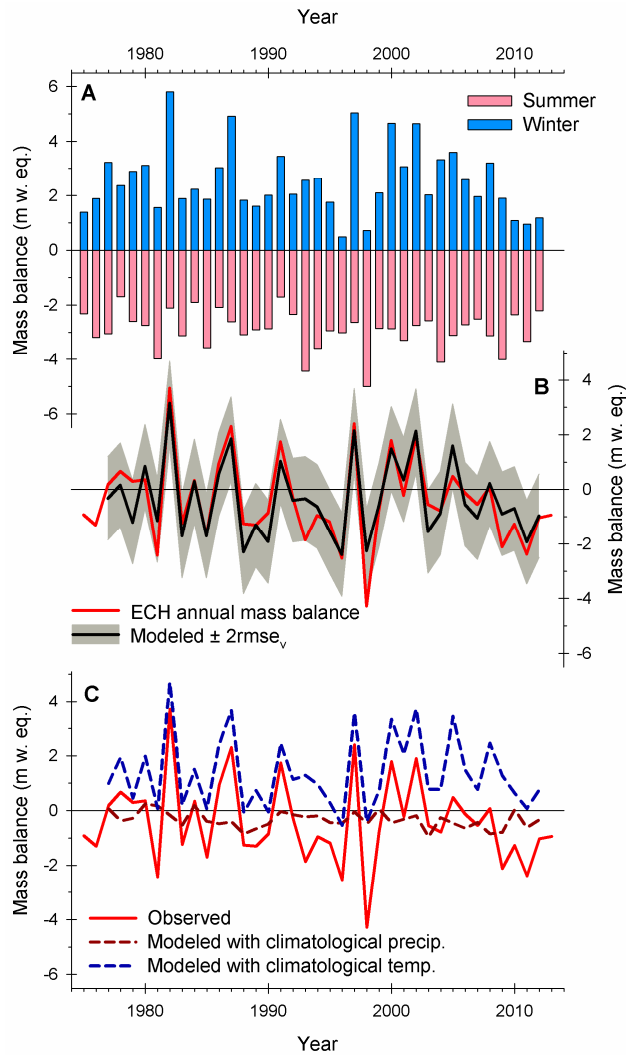
664



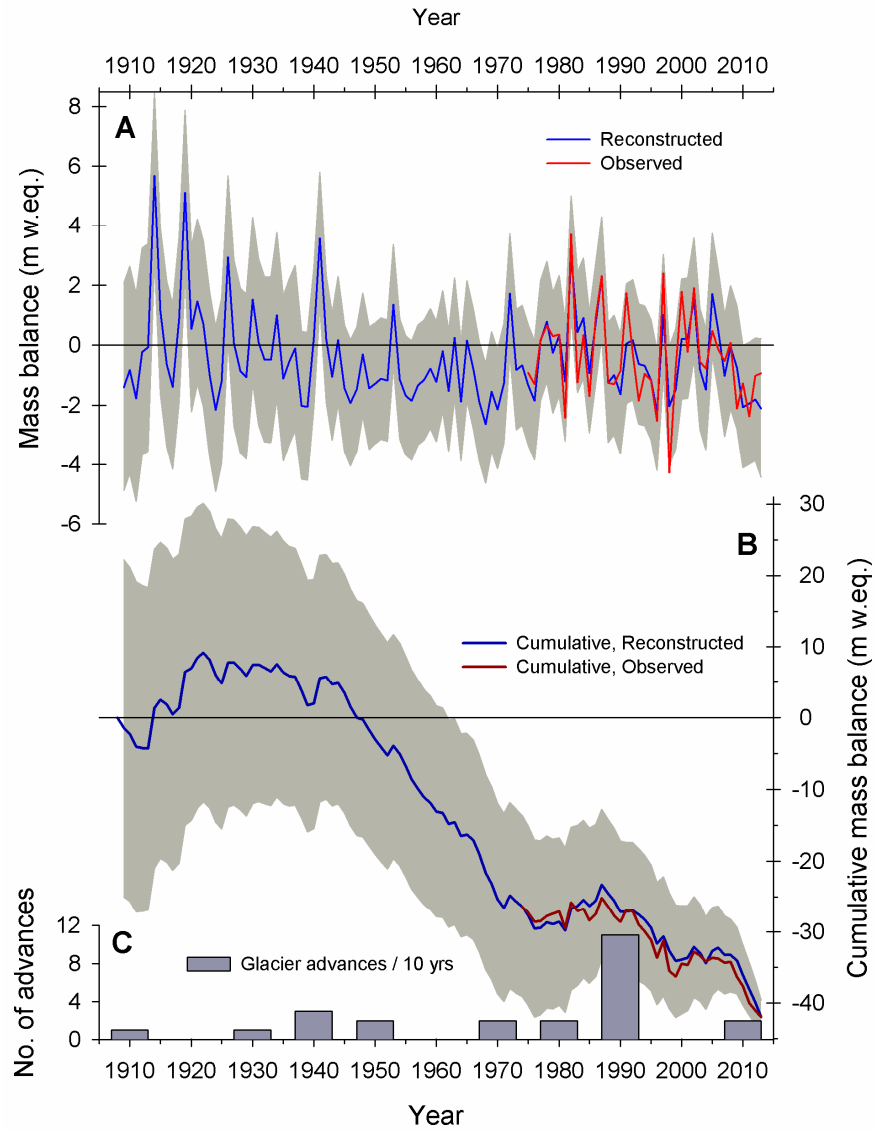
665
 666 **Figure 1. A)** Map of the Central Andes of Chile and Argentina showing the location of glaci-
 667 Echaurren Norte (ECH), glaciar Piloto Este (PIL), and several smaller glaciers with mass balance
 668 records in the Pascua Lama (PAS) and Cordillera de Colanguil (COL) areas. The locations of the
 669 snowpack and streamflow stations discussed in the text are also shown (Tables 1 and 2). **B)**
 670 General view of the El Yeso area, showing the location of ECH, El Yeso Dam, and the associated
 671 meteorological station. Laguna Negra is a natural lake that receives the meltwater from ECH.
 672 Base image acquired on January 5, 2014 and downloaded from Google Earth. **C)** Closer 3D view
 673 of glaciar Echaurren Norte as observed in 2014 and in the early 1970s (outlined in red and based
 674 on Peña and Narbona 1978). Note that the glacier has remained in roughly the same position but
 675 has thinned markedly over the last decades. **D)** Seasonal variations in temperature and
 676 precipitation at the lower reaches of ECH (3700 m asl) extrapolated from the El Yeso
 677 meteorological station (see section 2.2 for details). Note that the bulk of precipitation occurs
 678 during the coldest months of the year (December-March precipitation only accounts for ~5% of
 679 the mean annual totals).



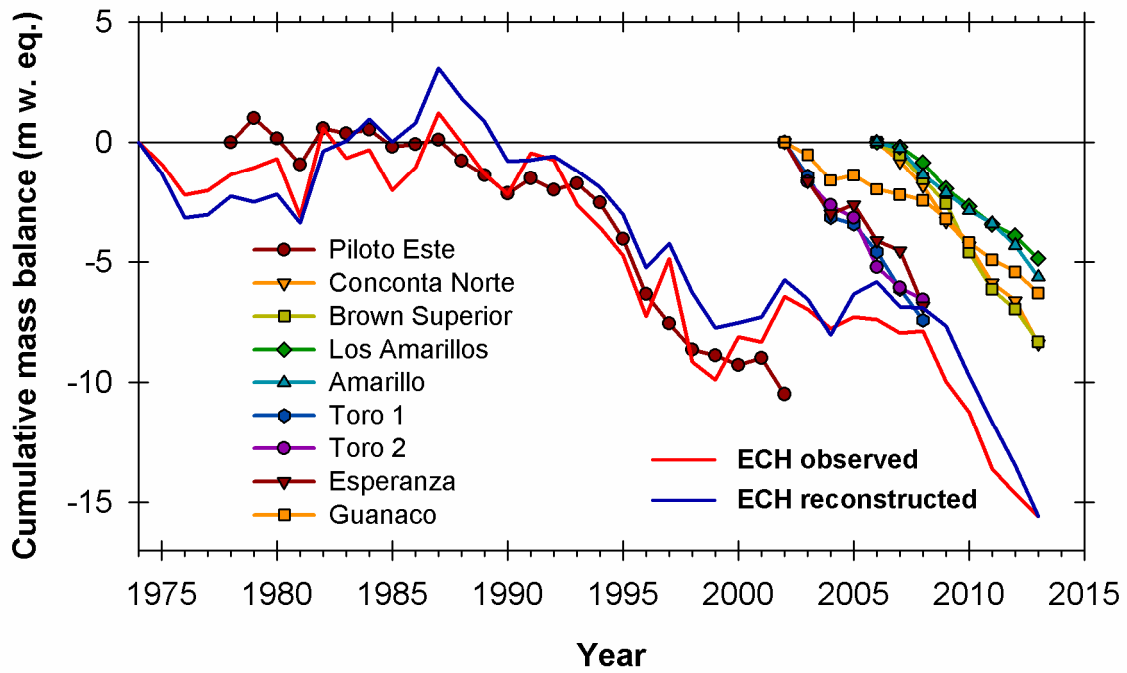
680
 681 **Figure 2.** Comparison between the annual mass balance series of ECH and regional records of
 682 maximum winter snow accumulation and mean annual river discharges in the Andes between 30°
 683 and 37°S (see Fig. 1). The regional records are expressed as percentages with respect to the 1981-
 684 2010 mean values. Variations in annual total precipitation at Santiago are also included to
 685 highlight the strong hydro-climatic signal in this region.



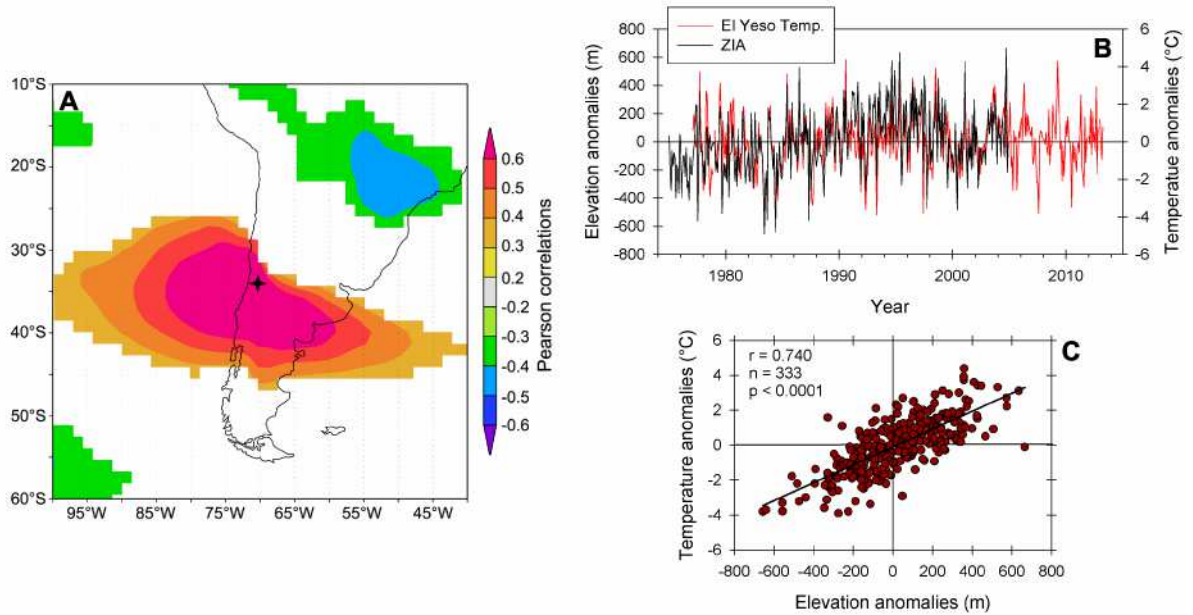
686
 687 **Figure 3.** (A) Winter and summer values observed at ECH between 1975 and 2012. (B) Annual
 688 mass balance series observed at ECH and modeled using El Yeso climate data (red and black
 689 lines, respectively). The estimated uncertainties of the modeled values (± 2 rmse) are shown with
 690 gray shading. (C) Annual mass balances observed at ECH (red line) compared to mass balances
 691 modeled using full variability in temperature but climatological monthly precipitation (dark red
 692 dashed line), and full variability in precipitation but climatological monthly temperatures (dark
 693 blue dashed line). Note the greater similarities between the observed series and the precipitation-
 694 based mass balance estimates.



695
 696 **Figure 4.** (A) Comparison between the annual mass balance record observed at ECH (red line)
 697 and the reconstructed series derived from regionally-averaged streamflow data (blue line). The
 698 estimated uncertainty of the reconstructed series ($\pm 2 \epsilon_{reco}$) is indicated by gray shading. (B)
 699 Cumulative record of the observed and reconstructed ECH mass balance series (dark red and dark
 700 blue lines, respectively). The initial value of the observed ECH cumulative record was modified
 701 to match the corresponding value in the reconstructed series. The aggregated errors in this series
 702 (see section 2.3) are also shown by gray shading (C) Glacier advances identified in the central
 703 Andes of Chile and Argentina during the past 100 years (see text for details). Events are grouped
 704 into 10-year intervals.



705
 706 **Figure 5.** Comparison between the cumulative patterns in the observed and reconstructed records
 707 from ECH and other glaciers with available direct mass balance data in the Dry Andes of Chile
 708 and Argentina (Fig. 1 and Table 1).



709
 710 **Figure 6.** A) Map showing the correlations ($p < 0.1$) between mean warm season (October-March)
 711 temperatures at the El Yeso station and gridded warm season ERA Interim mean temperatures for
 712 the 700 mb geopotential height level over the 1979-2012 period. The black star marks the
 713 location of the El Yeso station. **B)** Diagram showing variations of mean monthly temperatures at
 714 El Yeso (1977-2013) and the mean monthly elevation of the 0°C isotherm (ZIA) derived from
 715 radiosonde data from the Quintero coastal station (1975-2004). To facilitate the comparison, both
 716 series are expressed as anomalies from their mean seasonal cycles. **C)** Scatterplot of the El Yeso
 717 temperature and ZIA anomalies depicted in B. Note the positive, highly significant correlation
 718 between these two variables. ZIA data were provided by J. Carrasco from Dirección
 719 Meteorológica de Chile.
 720